



Available online at www.sciencedirect.com

ScienceDirect



Nuclear Physics A 1005 (2021) 121925

www.elsevier.com/locate/nuclphysa

XXVIIIth International Conference on Ultrarelativistic Nucleus-Nucleus Collisions (Quark Matter 2019)

Highlights from the PHENIX Collaboration

Megan Connors for the PHENIX Collaboration^{a,b}

^aDepartment of Physics and Astronomy, Georgia State University, Atlanta, GA
^bRIKEN BNL Research Center, Upton, NY

Abstract

PHENIX presented several new results at Quark Matter 2019 in 7 parallel talks and 7 posters. These proceedings highlight a sampling of the measurements presented during the conference. PHENIX results on flow in small systems, published in Nature Physics, indicate that the flow in small systems is driven by the initial state geometry. Additional measurements exploring QGP effects in small systems have also been explored. Two-particle correlations in d+Au and 3 He+Au suggest potential modification compared to those in p+p collisions. PHENIX has also measured J/Ψ in the forward and backward rapidity regions in d+Au and 3 He+Au collisions. Thermal photon measurements are also consistent with QGP formation in small systems. A new measurement of thermal photons using the Au+Au data set collected by PHENIX in 2014 verifies the scaling relationship previously observed for thermal photons. New results for a variety of hadron species with increasing precsion are now available and provide both insight into hadronization as well as crucial information for energy loss models that use R_{AA} to tune their parameters. Jet modification is also studied via a new observable extracted from π^0 -hadron correlations in Au+Au collisions.

Keywords: heavy-ion, QGP, small systems, flow

1. Evidence for QGP in Small Systems

1.1. Flow and initial state geometry

PHENIX has published measurements of the second and third Fourier coefficients referred to as v_2 and v_3 used to describe the azimuthal distribution of final-state particles produced in p+Au, d+Au, and 3 He+Au collisions which create intrinsically circular, elliptic and triangular initial geometries respectively [9]. In heavy-ion collisions the coefficients, v_2 and v_3 , are found to correspond to the elliptic and triangular flow. The measurements in these three smaller collision systems were possible due to the versatility of RHIC which enabled us to modify the initial state geometry of the small systems to discriminate between mechanisms driving the flow observed in small collision systems at RHIC and the LHC. According to a Glauber model Monte Carlo calculation, the second order eccentricity for p+Au is less than in d/ 3 He+Au collisions while the third order eccentricity for 3 He+Au is larger than the p/d+Au collisions. PHENIX observed a smaller v_2 in p+Au than the other two systems and a larger v_3 in the 3 He+Au system. These results indicate a clear correlation between the observed v_n flow terms and the initial state geometry. Thus

far, only hydrodynamic calculations such as those shown in Figure 1 which include QGP formation have been able to describe all this data simultaneously [10].

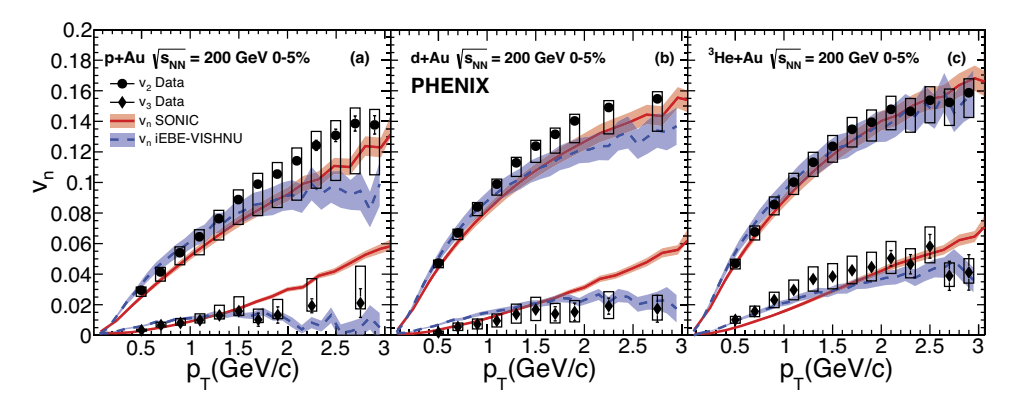


Fig. 1. The v_2 (circles) and v_3 (diamonds) of charged hadrons in 0-5% 200 GeV (a) p+Au, (b) d+Au and (c) 3 He+Au collisions and compared to hydrodynamic calculations[9]. Vertical bars and open boxes indicate the statistical systematic uncertainties respectively.

In addition to models, which indicate the temperatures achieved in the central collisions for small systems is high enough for QGP formation [10], evidence of thermal photons measured by PHENIX support this conclusion as well. For larger systems a scaling relationship has been reported across various collision species and collision energies [11]. The integrated photon yield is well described by the functional form functional form $A(dN_{ch}/d\eta)^{\alpha}$ where α was found to be 1.25. Figure 2 shows how the integrated photon yield as a function of the charge tracked multiplicity in the p+Au and d+Au compares to the larger A+A systems. There appears to be a smooth trend from the A+A scale to the pQCD calculations, which could indicate the multiplicities at which QGP effects turn on.

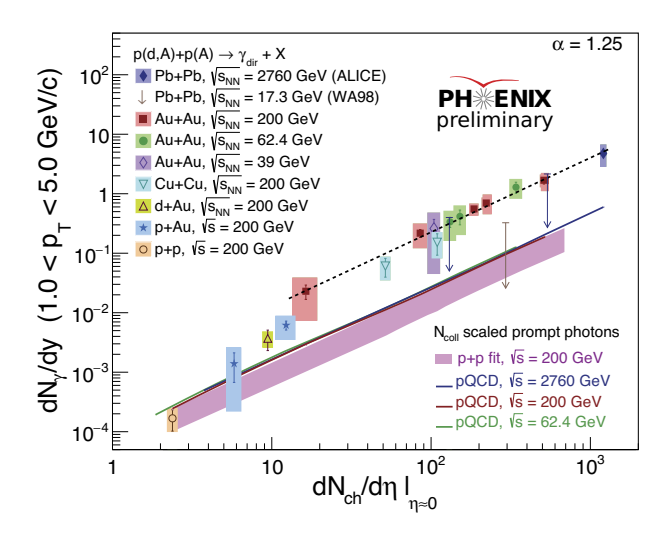


Fig. 2. Integrated yield of photons in a variety of collision systems including p+Au and d+Au as a function of $dN_{ch}/d\eta$. A fit to the A+A with a slope of $\alpha=1.25$ (dashed) and pQCD predictions (solid lines) are shown. The band, an extension of the p+p data point (open circle), agrees with the pQCD expectations. Vertical bars and shaded boxes indicate the statistical and systematic uncertainties respectively.

1.2. QGP signatures at high p_T

PHENIX measurements of jet spectra and π^0 spectra at high p_T in central d+Au collisions show suppression. As shown in Figure 3, this suppression has now also been observed for π^0 s above 8 GeV/c in p+Au and 3 He+Au collisions. Comparing the mean R_{AB} at high p_T in these systems to that in p+Al, reveals that the level of suppression is independent of the nuclei being traversed. This is different from the mean R_{AB} in the 4-6 GeV/c momentum range which appears to scale with the number of binary collisions, N_{Coll} .

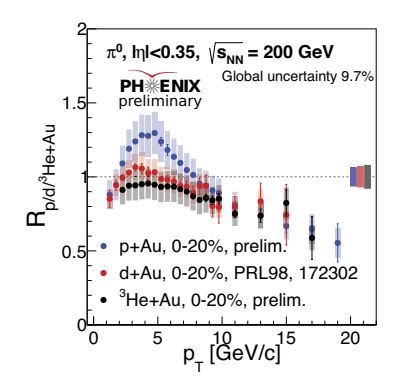


Fig. 3. The nuclear modification factor of π^0 spectra in p+Au, d+Au and 3 He+Au collisions at 200 GeV. Vertical bars indicate the statistical uncertainty and shaded boxes on each point indicate the systematic uncertainties. Shaded bands on the right side of the plot indicate the global scale uncertainty for each dataset

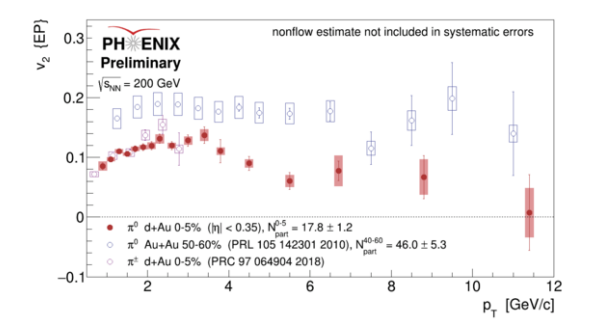


Fig. 4. The v_2 of neutral (solid circles) and charged (open pink circles) pions in 0-5% d+Au collisions at 200 GeV compared to v_2 of neutral (open blue circles) 50-60% central Au+Au collisions at 200 GeV. Vertical bars indicate the statistical uncertainty and open or shaded boxes on each point indicate the systematic uncertainties.

While alternative theories have been proposed to explain the data, other probes that may be sensitive to final state energy loss are explored. PHENIX has extended the previously published π^0 v_2 measurements in d+Au collisions to higher π^0 p_T values as shown in Figure 4. At low p_T the new measurement is consistent with the published results. At high p_T the π^0 v_2 appears non-zero up to 10 GeV/c. While elliptic flow drives the v_2 signal at lower momenta, the non-zero v_2 at high p_T observed in the Au+Au data also shown in Figure 4 is attributed to pathlength dependent energy loss. It is interesting to speculate if this signal in d+Au is indicative of energy loss effects in small systems or if alternative explanations can describe the data.

To further probe for potential energy loss effects in small systems, PHENIX studies π^0 -hadron correlations using π^0 s with $p_T > 5$ GeV/c as trigger particles. The angular distance along the azimuthal direction between the trigger π^0 and all hadrons in the event are measured and corrected for detector effects. The yield of π^0 -hadron pairs as a function of $\Delta\phi$ has a peak about $\Delta\phi=0$ corresponding to the jet that includes the π^0 trigger, called the nearside and a peak about $\Delta\phi=\pi$ corresponding to the jet opposing the π^0 , called the awayside. The integrated yield in 0-20% central d+Au collisions is compared to that in p+p via the ratio called I_{dA} which is defined as

$$I_{xA} = \frac{Y_{xAu}^{Away}}{Y_{pp}^{Away}} \tag{1}$$

The awayside I_{dA} is shown in Figure 5 as a function of $z_T = p_T^h/p_T^{\pi^0}$. A slight suppression is observed for $z_T > 0.3$ which would be consistent with energy loss. In A+A, along with suppression at high z_T , an enhancement is observed at low z_T . There is a hint of enhancement in the I_{dA} at low z_T but it is consistent with unity within the systematic uncertainties. To reduce the systematic uncertainties, another ratio,

$$R_{I} = \frac{Y_{xAu}^{Away}/Y_{xAu}^{Near}}{Y_{nn}^{Away}/Y_{nn}^{Near}},$$
(2)

divides the awayside I_{dA} by the nearside I_{dA} . R_I has been measured in ${}^3\text{He+Au}$ and is shown in Figure 6. Both collision systems exhibit a similar trend. The ratio of R_I in ${}^3\text{He+Au}$ over that in d+Au is shown in Figure 7. A fit to the ratio at high z_T is shown in the figure and gives an average value 0.876 +/- 0.061) that is 2 sigma below 1 indicates a slightly stronger suppression in ${}^3\text{He+Au}$ which would be consistent with additional energy loss in the larger system.

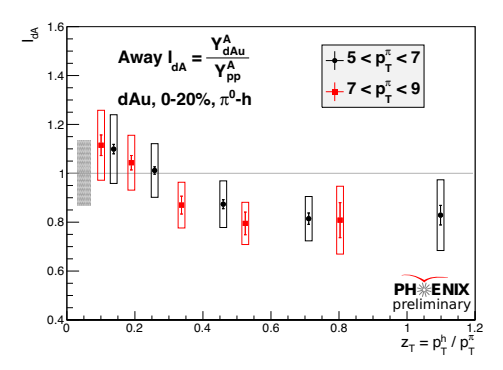


Fig. 5. Awayside I_{dA} for 0-20% central d+Au collisions. Vertical bars indicate the statistical uncertainty and boxes on each point indicate the systematic uncertainties. A shaded band on the left side of the plot indicates the global scale uncertainty.

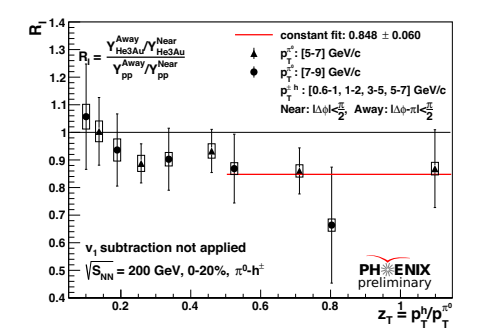


Fig. 6. R_I as a function of z_T for 0-20% central 3 He+Au collisions. Vertical bars and boxes indicate the statistical and systematic uncertainties respectively.

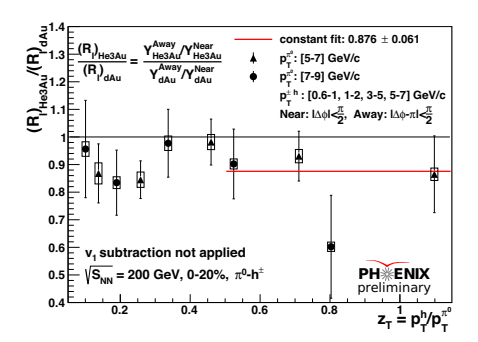


Fig. 7. The R_I as a function of z_T . Vertical bars and boxes indicate the statistical and systematic uncertainties respectively.

1.3. Quarkonia in small systems

 J/Ψ has been measured in the forward and backward rapidity regions in p+Al, p+Au and 3 He+Au collisions [1]. A new reweighted shadowing model is able to reproduced the observed modifications at forward rapidity while for backward rapidity it is necessary to include absorption in the model to properly describe the data. However, the model fails to describe the centrality dependence of the suppression observed in the forward rapidity region. For central p+Au collisions, a very strong suppression is observed in the forward rapidities compared to peripheral collisions while the R_{AB} at backward rapidity is independent of collision centrality. For both the forward and backward rapidities a p_T dependence is observed as shown in Figure 8. When comparing the p+Au and 3 He+Au collisions, the the ratio is consistent with unity within the systematic uncertainties but there is a hint that the effect may be stronger for the 3 He+Au system which would be consistent with QGP formation. Additional quarkonia measurements may be able to provide more insight.

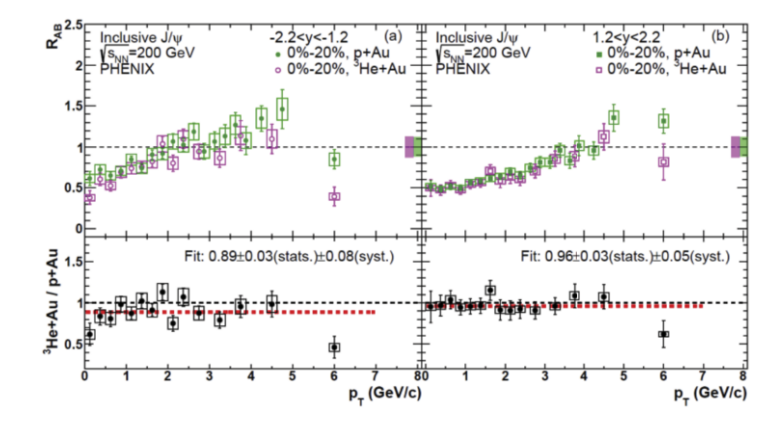


Fig. 8. R_{AB} of inclusive J/Ψ in p+Au (solid markers) and 3 He+Au (open markers) for backward (left) and forward (right) rapidity ranges. The ratio comparing the two collisions systems are plotted in the bottom panels. Vertical bars and boxes indicate the statistical and systematic uncertainties respectively. Shaded bands on the right side of each plot indicate the global scale uncertainties.

2. QGP in Heavy Ion Collisions

2.1. R_{AA}

During the first 16 years of RHIC running, PHENIX recorded data in a variety of collision systems which enables us to measure how the modification of particle spectra depends on system size. In addition, QGP effects on particle composition can be studied by measuring a variety of particle species. Figure 9 shows the p_T dependence for a variety of mesons in Cu+Au collisions for several slices of centrality. At lower p_T the ϕ meson is less suppressed than lighter mesons. This was also observed in U+U collisions. In Cu+Au collisions, K^* was found to be suppressed by the same factor as for the ϕ which may indicate the role of strangeness in the nuclear modification factor.

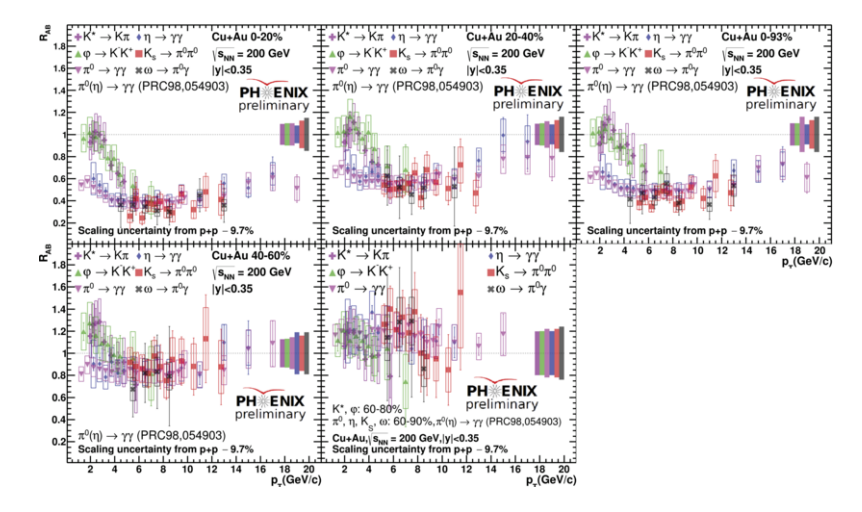


Fig. 9. R_{AB} for various mesons measured in Cu+Au collisions. Each panel shows a different centrality class. Vertical bars and boxes on each point indicate the statistical and systematic uncertainties respectively. Shaded bands to the right of each plot indicate the corresponding global scale uncertainty.

Figure 10 shows that protons are clearly enhanced in Cu+Au and that the R_{AB} measured for protons

in Cu+Au is consistent with that measured in Au+Au collisions when selecting events with similar N_{part} . Figure 11 shows the average meson and proton R_{AB} as a function of N_{part} . These results suggest that the interplay of radial flow, strangeness and recombination is different in the large A+A systems compared to the smaller collision systems [5].

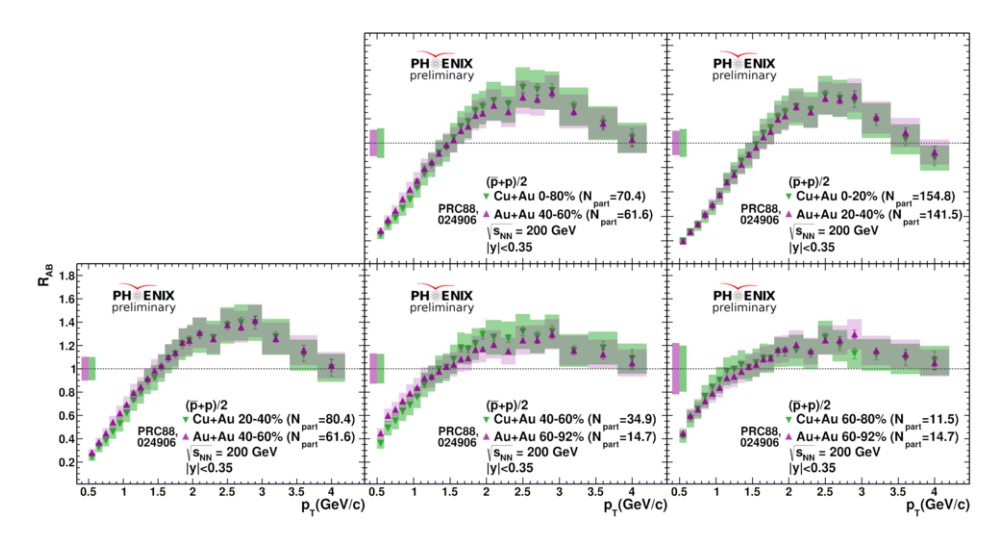


Fig. 10. R_{AB} for protons in Cu+Au and Au+Au collisions compared for similar N_{part} values. Vertical bars indicate the statistical uncertainty and shaded boxes on each point indicate the systematic uncertainties. Shaded bands on the left side of each plot indicate the global scale uncertainty for each dataset.

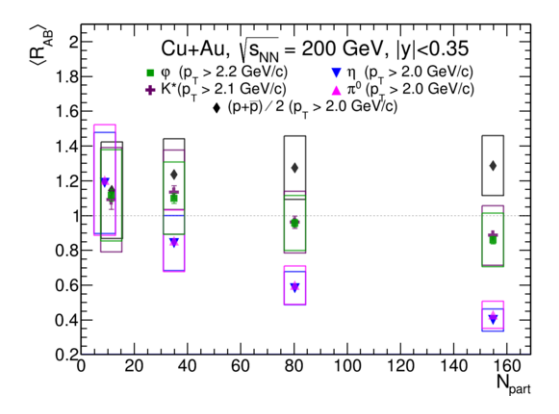


Fig. 11. The average R_{AB} for a variety of hadron species with $p_T > 2$ GeV/c in Cu+Au collisions as a function of N_{part} . Vertical bars indicate the statistical uncertainty and shaded boxes on each point indicate the systematic uncertainties.

In Figure 9 the R_{AB} for different particles converge at $p_T > 5$ GeV/c. For higher momentum particles, energy loss is the dominant mechanism causing the observed suppression. Figure 12 shows the average R_{AA} for a variety of high momentum ($p_T > 5$ GeV/c or $p_T > 6$ GeV/c) particles as a function of N_{part} . Data from U+U, Au+Au and Cu+Cu collisions which $\sqrt{s_{NN}} \approx 200$ GeV are included in the figure. This suppression is independent of particle species and the collision system. Precise R_{AA} measurements are crucial for energy loss models that use them to tune their parameters before comparing to other energy loss observables.

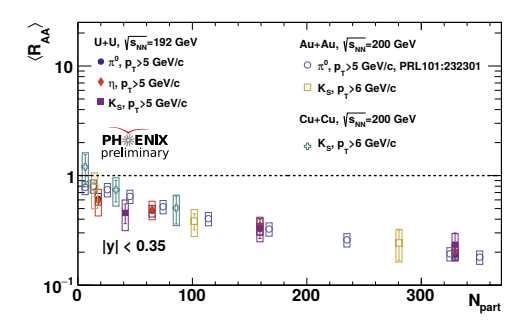


Fig. 12. The nuclear modification factor of several mesons in U+U, Au+Au and Cu+Cu collisions. Vertical bars and boxes indicate the statistical and systematic uncertainties respectively.

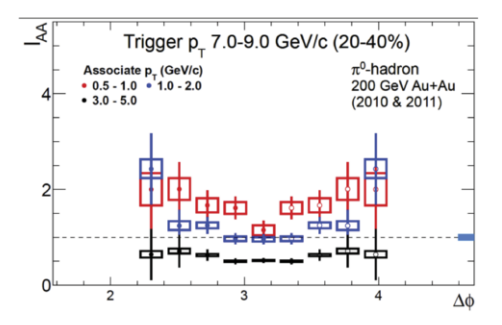


Fig. 13. The I_{AA} as a function of $\Delta \phi$. Vertical bars and open boxes indicate the statistical and systematic uncertainties respectively. A shaded band on the right side of the plot indicates the global scale uncertainty.

2.2. π^0 -hadron correlations

While R_{AA} provides insight to the average energy loss in the QGP, more differential observables such as two-particle correlations, which use di-jets to study jet modification, impose important constraints on energy loss models and improve our understanding of how the lost energy is redistributed. PHENIX reports new results from π^0 -hadron correlations using π^0 s with $p_T > 4$ GeV/c as trigger particles. The modification to the particle composition and shape of the jet opposing the trigger particle, can be studied by comparing the conditional yield Y^{Away} and width of the awayside peak in Au+Au to p+p.

The awayside I_{AA} which is defined in 1 is plotted as function of $\Delta\phi$ in Figure 13 for π^0 -hadron correlations using π^0 triggers with p_T 7-9 GeV/c. This is a proxy for measuring modifications to the fragmentation function, $D(p_T)$, as a function of the distance from the jet axis. In the case of the di-hadron correlations the jet axis is approximated as directly π from the trigger particle. The I_{AA} for associated particles with $p_T > 3$ GeV/c shows constant suppression at all angles. However for lower momentum particles there is a clear enhancement which is most prominent at wider angles from the jet axis. This is consistent with gluon Bremstralung but these measurements can further constrain energy loss models.

2.3. Direct Photons

As shown in Figure 14 and reported previously, the integrated yield of direct photons plotted as a function of $dN_{ch}/d\eta$ appear to lie on a power law curve with exponent $\alpha=1.25$. However, the yields reported by the STAR collaboration lie below this trend. During this conference, PHENIX showed results using a different method to extract the photon yield in Au+Au collisions with the 2014 data set. The previous PHENIX measurements used the electromagnetic calorimeters (EMCal) to identify photons while the new results use internal conversions. Figure 14 shows excellent agreement between the two PHENIX measurements and provides further evidence of this scaling relationship.

3. Summary and Outlook

These proceedings focus on the mounting evidence for QGP formation in small systems and recent measurements to quantify the QGP in A+A systems. PHENIX results on flow in small systems, published in [9], indicate that the flow in small systems is driven by the initial state geometry [6]. Additional measurements exploring QGP effects in small systems have also been explored. Two-particle correlations in d+Au and 3 He+Au suggest potential modification compared to those in p+p collisions [2]. PHENIX has also measured J/Ψ in the forward and backward rapidity regions in d+Au and 3 He+Au collisions [1]. Thermal photon measurements are also consistent with QGP formation in small systems. A new measurement of thermal photons using the Au+Au data set collected by PHENIX in 2014 verifies the scaling relationship

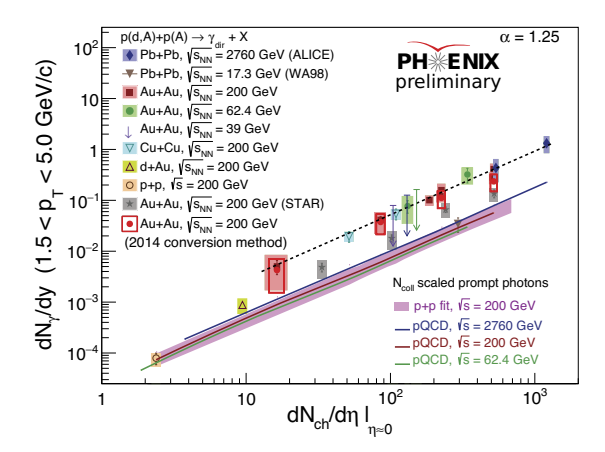


Fig. 14. The integrated yield of photons in a variety of collision systems including the new Au+Au results using the conversion method.

previously observed for photon yield [3]. New results for a variety of hadron species with increasing precsion are presented and provide insight into hadronization and crucial input for energy loss models that use R_{AA} to tune their parameters. The first measurement of I_{AA} as a function of $\Delta \phi$ for π^0 -h correlations in Au+Au demonstrates how the lost energy is redistributed within the jet [7]. In addition, PHENIX presented results on heavy flavor [4] and spectra in small systems [5] at QM2019.

PHENIX continues to report new impactful results which utilize the unique strengths of its detector system such as the finely segmented EMCal enabling precise direct photon and electron measurements at mid-rapidity, the muon arms at high rapidity, and vertex detectors spanning different rapidity ranges. PHENIX plans to further investigate the effects observed for J/Ψ at forward and backward rapidities in small asymmetric collision systems by measuring $\Psi(2S)$ in these same collisions and rapidity ranges. Further confirmation of our understanding of small system, can be performed by verifying the N_{coll} scaling with direct photon measurements in small systems. In addition to the wealth of R_{AA} measurements for a variety of particle species and collision systems, PHENIX will publish the charm and bottom separated R_{AA} and v_2 . Using the higher statistic Au+Au data collected in 2014 and 2016, the new π^0 -h correlations presented will be extended to the direct photon tagged correlations in which the photon give access to the initial kinematics.

4. Acknowledgements

The author acknowledges support from the National Science Foundation and the RIKEN BNL Research Center for her work in addition to the acknowledgments included in the PHENIX author list.

References

- [1] K. Smith for the PHENIX Collaboration, these proceedings
- [2] J. Runchey for the PHENIX Collaboration, these proceedings
- [3] W. Fan for the PHENIX Collaboration, these proceedings
- [4] T. Todoroki for the PHENIX Collaboration, these proceedings
- [5] I. Mitrankov for the PHENIX Collaboration, these proceedings
- [6] S. Han for the PHENIX Collaboration, these proceedings
- [7] A. Hodges for the PHENIX Collaboration, these proceedings
- [8] U. A. Acharya, et. al, Measurement of J/Ψ at forward and backward rapidity in p+p, p+Al, p+Au, and 3 He+Au collisions at $\sqrt{s_{NN}} = 200$ GeV, arXiv: 1910.14487[hep ex] (2019).
- [9] C. Aidala, et. al, Creation of quark-gluon plasma droplets with three distinct geometries", Nature Physics 15 (2019) 214 220.
- [10] C.Shen, et. al, Collectivity and electromagnetic radiation in small systems, *Phys.Rev.C* 95 (1) (2017) 014906.
- [11] A. Adare et al., Beam Energy and Centrality Dependence of Direct-Photon Emission from Ultrarelativistic Heavy-Ion Collisions, Phys.Rev.Lett. 123, (2019) 022301.